$(d,{}^{6}\text{Li})$ reaction on ${}^{24}\text{Mg}$ and ${}^{26}\text{Mg}$ at $E_d = 80$ MeV

W. Oelert, W. Chung, A. Djaloeis, C. Mayer-Böricke, and P. Turek

Institut für Kernphysik, Kernforschungsanlage Jülich, D—5170 Jülich, West Germany
(Received 20 February 1980)

The $(d,{}^{6}\text{Li})$ reaction on ${}^{24}\text{Mg}$ and ${}^{26}\text{Mg}$ has been measured at a bombarding energy of 80 MeV. Angular distributions were obtained in an angular range of 6° (2° for the ground state transitions) to 35° lab. Experimentally an excitation energy range up to 30 MeV was observed. In the framework of finite-range distorted-wave Born approximation calculations α spectroscopic factors were extracted and compared to recent shell-model predictions.

> NUCLEAR REACTIONS ${}^{24}\text{Mg}(d,{}^{6}\text{Li}){}^{20}\text{Ne}$, ${}^{26}\text{Mg}(d,{}^{6}\text{Li}){}^{22}\text{Ne}$. $E_d = 80$ MeV, measured $\sigma(E_{{}^{6}\text{Li}}, \theta)$. Enriched targets. Finite-range DWBA calculations. Deduced alpha spectroscopic factors.

I. INTRODUCTION

During the last decade interest in nucleon correlations has increased rapidly.[1-8] Many contributions have been published concerning multi- and few-nucleon transfer reactions, especially four-nucleon transfer studies.

The effort of extracting quantitative information on spectroscopic strength distributions of four-nucleon correlations in nuclei has been mutually stimulated by recent theoretical development and experimental progress. Theoretical calculations have been performed in the framework of the SU_3 model,[9-12] the pairing-vibrational model,[13-15] the interacting boson approximation,[16,17] the cluster description,[11,18-21] and the shell model.[11,22-25]

To compare experimental and theoretical results it appears to be necessary on the experimental side of the problem to (i) determine the strength of the different parts of the reaction mechanism involved in the yield of a measured transfer reaction cross section, (ii) understand the reaction mechanism for the population of an individual final state as, e.g., to distinguish between direct cluster and sequential transfer, and (iii) have at least a consistent prescription on how to extract the spectroscopic strength from the measured cross section, since absolute and relative experimental spectroscopic factors appear to be model dependent.

In this contribution we present results on measurements of the four-nucleon transfer reaction $(d,{}^{6}\text{Li})$ on ${}^{24}\text{Mg}$ and ${}^{26}\text{Mg}$ leading to ${}^{20}\text{Ne}$ and ${}^{22}\text{Ne}$, respectively. An analysis of our data in the framework of finite-range distorted-wave Born-approximation (FR-DWBA) is given and the results are compared to recent predictions of shell-model calculations.[25,26] Investigations of the

${}^{24}\text{Mg}(d,{}^{6}\text{Li})$ (Refs. 27–35) and of the ${}^{26}\text{Mg}(d,{}^{6}\text{Li})$ (Refs. 32, 33, 35) reactions have been carried out previously at various deuteron energies and are compared to the present results.

II. EXPERIMENTAL PROCEDURE

The 80 MeV deuteron beam from the Jülich Isochronous Cyclotron JULIC was used to measure angular distributions of the $(d,{}^{6}\text{Li})$ reaction on the isotopes ${}^{24}\text{Mg}$ and ${}^{26}\text{Mg}$. Typical energy spectra are shown in Figs. 1 and 2. The angular range for detecting the reaction products was typically 8°–35° lab. Additional data points at angles lower than 7° lab for the ground-state transitions ${}^{24,26}\text{Mg}(d,{}^{6}\text{Li}){}^{20,22}\text{Ne}_{g.s.}$ were taken using a double-focusing magnetic analyzer of low dispersion.[36] The experiments were performed using conventional ΔE-E surface barrier detector techniques. Two to three telescopes were used during
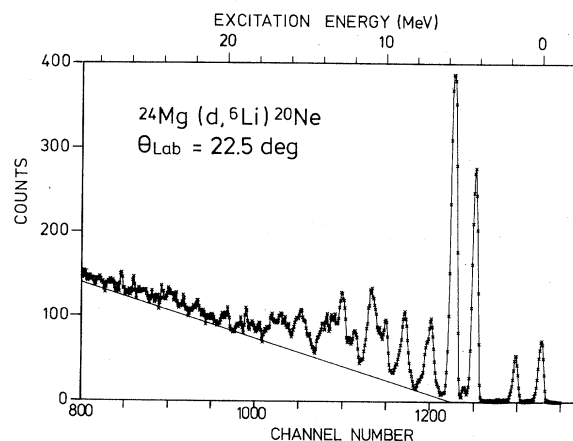

FIG. 1. Energy spectrum of the $(d, {}^{6}\text{Li})$ reaction on ${}^{24}\text{Mg}$. The straight line indicates a supposed continuous background.
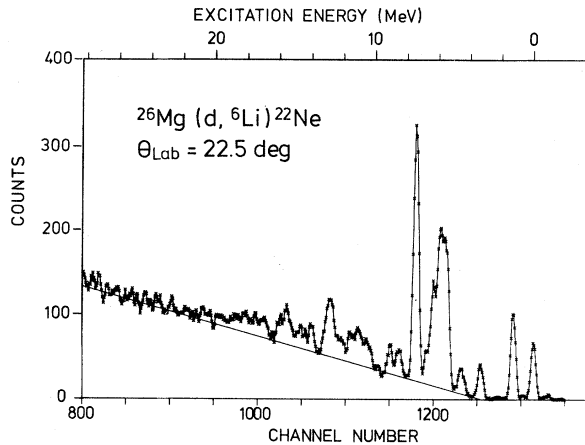
FIG. 2. Energy spectrum of the $(d, {}^{6}Li)$ reaction on ${}^{26}Mg$. The straight line indicates a supposed continuous background.

the various experiments; the thicknesses of the ΔE and E detectors were 100–200 μm and 1000–2000 μm, respectively. The particle identification was sufficient to ensure separation between the outgoing ${}^{6}Li$ and ${}^{7}Li$ ions, covering an "excitation energy range" of up to 30 MeV. However, since only singles energy spectra were measured, the extent to which final states of the nuclei ${}^{20}Ne$ or ${}^{22}Ne$, respectively, were observed at excitation energies above the particle decay threshold was not determined in the present experiment [Q-values: ${}^{20}Ne(\gamma, \alpha) = 4.7$ MeV, ${}^{22}Ne(\gamma, \alpha) = 9.7$ MeV].

Self-supporting foils were used as targets with the target thicknesses between 370 and 775 μg/cm^{2}. The isotopical enrichment of ${}^{24}Mg$ and ${}^{26}Mg$ was 99.96% and 97.10%, respectively. Only a minor yield accounting from the ${}^{16}O$ impurity in the target was observed in some energy spectra, identified by the kinematic shift. Since angular distributions for the ${}^{16}O(d, {}^{6}Li){}^{12}C$ reaction have been measured at 80 MeV deuteron energy[37] the ${}^{16}O(d, {}^{6}Li){}^{12}C$ impurity yield could be accounted for by subtraction whenever it was necessary. The target thicknesses have been determined by weighing and by alpha-particle energy loss measurements; both results agreed within 5%. At least the relative accuracy of this method was verified since different targets had been used during the various runs and overlapping angular ranges were always measured. The incident beam was continuously monitored by a Ge(Li) detector at an angle of 30° lab relative to the beam direction. The ratio of the deuteron yield elastically scattered into the monitor counter and the integrated charge collected in a Faraday cup was used to ensure the accuracy of the determination of the cross section at the various

angles during one experiment. The absolute cross sections were determined by the integrated charge only and are believed to be accurate to within 15%, except for the cases where the uncertainties arising from counting statistics and background subtraction are larger.

Because of the rather low cross sections, a high intensity achromatic beam was used ranging from 0.02 to 2 μA on the target, depending on the reaction angle. An overall energy resolution of 300 keV full width at half maximum (FWHM) was typical for the ${}^{6}Li$ spectra. In addition, some spectra were taken with a low intensity dispersive beam, resulting in an energy resolution of 160 keV FWHM.

The extraction of the yields of the observed peaks was done employing the computer code Autofit.[38] This way it was possible in some cases to disentangle the yields of peaks which are due to the excitation of unresolved doublets or triplets, as they can be observed in the energy spectra, Figs. 1 and 2. The present data were analyzed up to an excitation energy of 12.6 and 9.1 MeV for the final nuclei ${}^{20}Ne$ and ${}^{22}Ne$, respectively.

III. THE SPECTROSCOPIC FACTORS

The experimental angular distributions were compared to FR-DWBA calculations to extract alpha-spectroscopic factors S_{α}. The DWBA code LOLA [39] was used in the post representation. Typical results of the DWBA calculations for the ${}^{24}Mg(d, {}^{6}Li)$ reaction to final states in ${}^{20}Ne$ are shown in Fig. 3. It appears that at the incident energy of $E_{d} = 80$ MeV, neighboring L transfers show similar shapes of the angular distributions. Consequently, the shape of the angular distribution cannot be used for a unique determination of spin and parity of final states at the present experimental conditions. This analysis is based on known spin and parity assignments, as given in Ref. 40 for ${}^{20}Ne$ and in Ref. 41 for ${}^{22}Ne$. For the particular case of $L = 2$ transfers it is shown in Fig. 3 that no strong dependence of the theoretical angular distribution shape on reaction Q values is observed (solid line: $E_{x} = 1.63$ MeV, dotted line: $E_{x} = 7.8$ Mev).

Deuteron[42] and ${}^{6}Li$ optical model potentials[43] were used as described in Ref. 44. Throughout this contribution the calculations done with the code LOLA[39] employed (i) no energy dependence of the ${}^{6}Li$ optical potential and (ii) only $1S$ contributions of the "α - d" $\equiv {}^{6}Li$ relative motion. A study of the ${}^{16}O(d, {}^{6}Li){}^{12}C$ reaction at different incident energies[45] resulted in (i) a possibly required energy dependent ${}^{6}Li$ optical potential
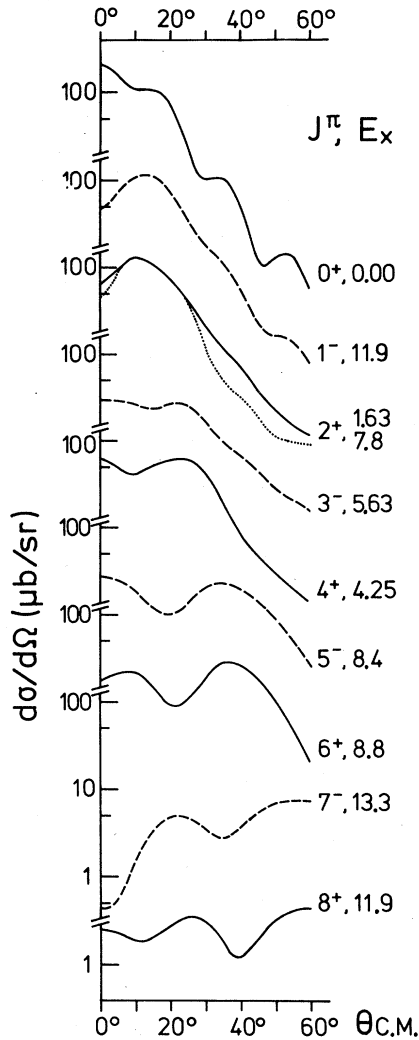
FIG. 3. DWBA calculations for angular distributions of the $(d, {}^6\text{Li})$ reaction of ${}^{24}\text{Mg}$ leading to natural parity states in ${}^{20}\text{Ne}$. The code LOLA (Ref. 39) was used.

and (ii) a possible necessary inclusion of $0D$ contributions to the $\alpha - d \equiv {}^6\text{Li}$ system. The finite-range DWBA code DWUCK5[46] was employed using (i) an energy dependence of the real volume part of the ${}^6\text{Li}$ optical potential as $dV_R/dE = -0.86$ with $V_R = -248$ and -240 MeV for the ${}^{24}\text{Mg}(d,{}^6\text{Li})$ and ${}^{26}\text{Mg}(d,{}^6\text{Li})$ reactions,[44] respectively, and (ii) a coherent superposition of $1S$ and $0D$ contributions for the relative motion of the $\alpha - d \equiv {}^6\text{Li}$ system, see Refs. 37, 45, and 47.

The bound-state wave functions of the α cluster (in the target nuclei and in the outgoing ${}^6\text{Li}$ particle) and the number of radial nodes in the wave functions were generated and used as described extensively in Refs. 37, 44, and 45).

Theoretical alpha-spectroscopic factors were

calculated with the method described by Bennett[48] from complete $d_{5/2}$-$s_{1/2}$-$d_{3/2}$ shell-model wave functions generated by the Chung-Wildenthal particle-hole interactions. For details of the calculations[25] we refer to Ref. 26.

IV. RESULTS

A. The ${}^{24}\text{Mg}(d,{}^6\text{Li}){}^{20}\text{Ne}$ reaction

The known natural, positive parity levels of ${}^{20}\text{Ne}$ (Ref. 40) are displayed in Fig. 4. The open circles which are connected by straight lines represent levels of the 0_1^+ ground-state band and of the 0_2^+ 6.72 MeV band. Both of them are built up predominantly of $(sd)^4$ nucleons outside the ${}^{16}\text{O}$ core. The calculated levels[26] (full circles) for these bands are easily identified with the equivalent experimental ones. Levels of the 0_3^+ band (open circles plus dots) are supposed to be of core excited nature $[(sd)^n(1p)^{4-n};\ 4 \leqslant n \leqslant 8]$ and are excited in the pickup reaction, but naturally they cannot be predicted by the sd-shell model calculations.[26] Finally, levels of the 0_4^+ band (crosses) predominantly include configurations of fp-shell contributions and are therefore neither predicted by the shell-model calculations nor excited in the present experiment with an observable yield.
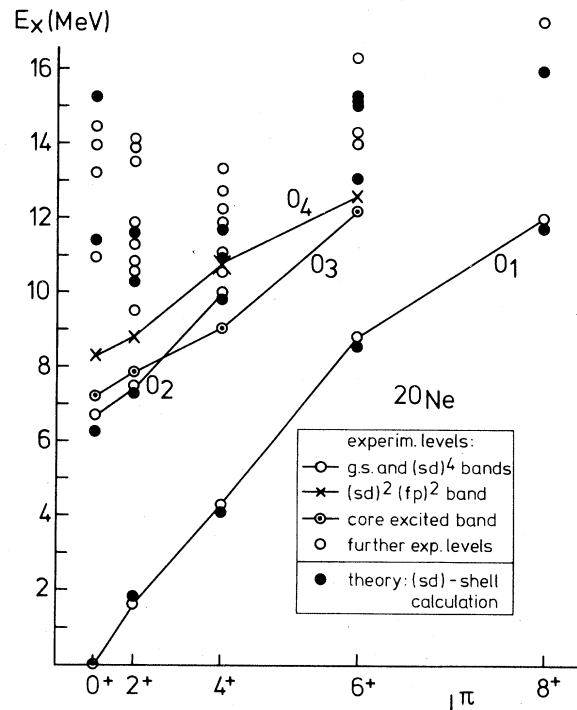

FIG. 4. Positive natural parity states in ${}^{20}\text{Ne}$; experimentally known levels and theoretically predicted ones.

The experimental angular distributions of the members of the gound-state band are shown in Fig. 5. The solid curves are FR-DWBA (LOLA)[39] calculations normalized to the experimental cross sections. In general, good agreement between the data and the theoretical curves is observed. The solid curves for the angular distributions to the observed peaks at 8.8 and 11.9 MeV were obtained by incoherent superposition of (i) $L = 1$ plus $L = 6$ (known[40]: 1^- states at 8.694 and 8.848

MeV, 6^+ state at 8.777 MeV) and (ii) $L = 1$, $L = 4$ plus $L = 8$ (known[40]: 1^- state at 11.962 MeV, 4^+ state at 11.926 MeV, 8^+ state at 11.949 MeV). The known 2^+ state at 11.866 MeV was not explicitly included for the fit, since $L = 1$ and $L = 2$ transfers reveal a rather similar angular distribution shape, see Fig. 3.

A disagreement between the experimental angular distribution shape and the DWBA prediction occurs for the case of the 4^+ state at 4.25 MeV. Even the FR-DWBA (DWUCK5)[46] calculations (dashed line), including an energy dependence of the ${}^6Li$ optical potential and $1S$- plus $0D$-state contributions of the α-$d \equiv {}^6Li$ relative motion, do not significantly improve the fit.

Based on experimental investigations[49] of α scattering on ${}^{20}Ne$, an antistretching effect has been suggested, resulting in an average separation distance between the ${}^{16}O$ core and the α particle being larger for the 6^+ than for the 8^+ state at 8.775 and 11.949 MeV, respectively.[50] In fact, a variation after projection Hartree-Fock calculation[51] shows that the rms radius of ${}^{20}Ne$ decreases with increasing spin of the ground-state band. DWBA calculations were performed in order to test a dependence of the theoretical angular distribution shape on the radius of the α-bound state (the calculations were done for the 4^+ state at 4.25 MeV in ${}^{20}Ne$). As shown in Fig. 6, the allowed flexibility of the radius does not change the shape of the theoretical angular distribution and consequently does not lead to an improvement of the fit to the experimental data; see Fig. 5.
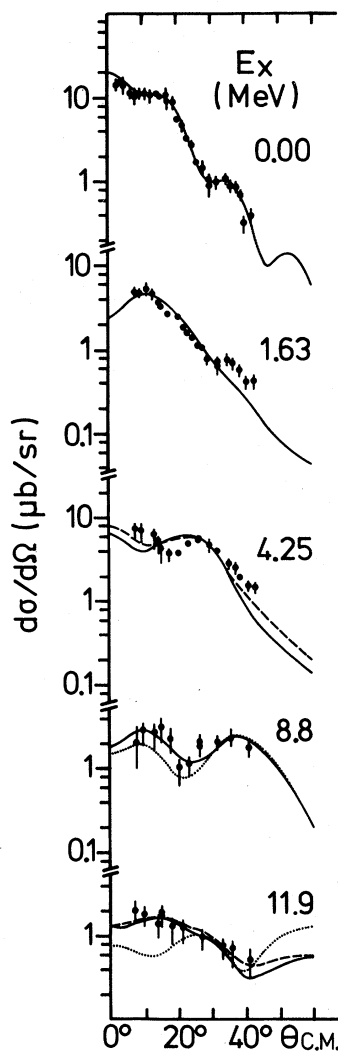

FIG. 5. Angular distributions of the $(d,{}^6Li)$ reaction for the members of the ground-state band in ${}^{20}Ne$. Solid lines: calculations done with the code LOLA, see text. Dashed lines: calculations done with the code DWUCK5, see text. The solid line for the 8.8 MeV angular distribution is a superposition of angular momentum transfers $L = 6$ plus $L = 1$; see Table I. The dotted line is a pure $L = 6$ DWBA curve. The solid and the dashed line for the 11.9 MeV angular distribution is a superposition of angular momentum transfer $L = 8$, $L = 4$, plus $L = 1$; see Table I. The dotted line is a pure $L = 8$ DWBA curve.
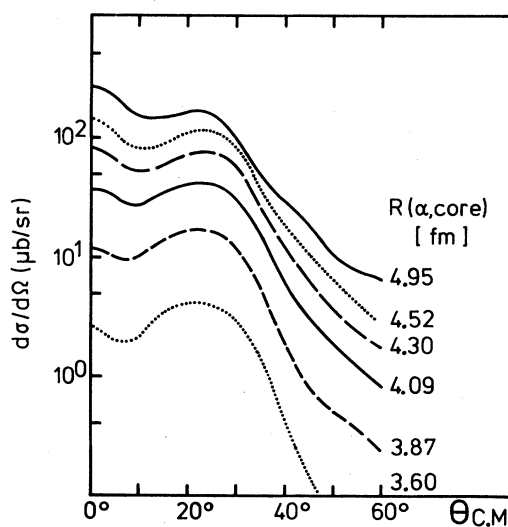

FIG. 6. DWBA angular distributions for the ${}^{24}Mg(d, {}^6Li){}^{20}Ne$ reaction leading to the 4^+ final state at 4.25 MeV excitation energy using various alpha-core radius parameters.

TABLE I. Alpha-spectroscopic factors S_α for final states in ^{20}Ne excited by the $(d, {}^6\text{Li})$ reaction. Values are presented from (i) sd-shell model calculations, (ii) the present analysis, and (iii) previous results. The S_α values for the ground-state transition is given relative to the $^{20}\text{Ne} \rightarrow {}^{16}\text{O}$ ground-state S_α factor; the others are relative to the $^{24}\text{Mg}(d, {}^6\text{Li}){}^{20}$Ne ground-state transition S_α factor. The label T is for $T=1$ final state in ^{20}Ne.

E_x(MeV) Ref. 40	J^π	Theory E_x(MeV) Ref. 26	S_α	Present experiment E_x(MeV)	S_α LOLA	S_α DWUCK5	Previous experiments S_α Ref. 35	S_α Ref. 34	S_α Ref. 32
0.000	0$^+$	0.00	0.59	0.00	0.45	0.53			
1.634	2$^+$	1.75	0.20	1.63	0.35	0.42	0.83	0.31	0.90
4.248	4$^+$	4.13	0.41	4.25	0.96^f	0.81^f	1.00	0.85	4.14
4.968	2$^-$			4.97					
5.621	3$^-$			5.63	3.81	4.32	3.08	3.09	1.24
5.784	1$^-$				0.95	0.84	0.25	0.42	0.19
6.724	0$^+$	6.24	0.09		<0.1^a		0.03		
7.004	4$^-$			6.95					
7.168	3$^-$				0.50	0.56		<0.74	
7.191	0$^+$			7.20	0.15^b	0.10^b	d	e	
7.421	2$^+$	7.37	0.01		<0.02^a		0.21	0.67	
7.829	2$^+$			7.80	0.10^b		d	e	
8.3	0$^+$								
8.449	5$^-$			8.4	0.6^f	0.5^f	1.08	1.98	
8.694	1$^-$				c	c	0.12		
8.777	6$^+$	8.54	0.71	8.8	0.82	0.62	1.92	7.04	
8.8	2$^+$								
8.848	1$^-$				c	c	0.06		
9.030	4$^+$				<0.05^{a,b}		d	e	
9.115	3$^-$						0.28		
9.318									
9.508	2$^+$	10.23	<0.01	9.4		<0.14^f			
9.873	3$^+$								
9.92	(1$^+$)								
9.99	4$^+$	9.86	0.20	10.0	0.43	0.37	0.35		
10.261	5$^-$					0.18			
10.272	2$^+$ T			10.3					
10.403	3$^-$					0.35			
10.548	4$^+$								
10.583	2$^+$						0.17		
10.609	6$^-$			10.6					
10.694	4$^-$3$^+$								
10.79	4$^+$								
10.838	3$^-$						0.21		
10.840	2$^+$					0.17	0.10		
10.89	3$^+$ T								
10.97	0$^+$	11.37	<0.01	10.9	weak				
11.015	4$^+$	10.97	0.13			0.17	0.30		
11.073	4$^+$ T								
11.23	1$^-$						0.11		
11.23	1$^+$ T								
11.256	1$^-$ T								
11.322	2$^+$	11.53	0.15				0.09		
11.528	3$^+$4$^-$								
11.552	(2$^+$0$^+$)								
11.555	1$^+$2$^-$3$^+$								
11.601	2$^-$ T								
11.656	(3$^+$)								
11.866	2$^+$						0.14		
11.926	4$^+$	11.70	0.02		0.08	0.07	0.34		
11.949	8$^+$	11.71	0.32	11.9	0.64	0.62			
11.962	1$^-$				0.11	0.17			

TABLE I. (Continued.)

E_x(MeV) Ref. 40	J^π	Theory E_x(MeV) Ref. 26	S_α	Present experiment E_x(MeV)	S_α LOLA	S_α DWUCK5	Previous experiments S_α Ref. 35	S_α Ref. 34	S_α Ref. 32
12.100	$2^- \, T$								
12.134	6^+								
12.215	$2^+ \, T$								
12.24	4^+								
12.254	$3^- 2^+$								
12.35	(2^+)								
12.39	$3^- \, T$			12.4	0.36^f	0.41^f	0.21		
12.412	(0^+)						0.02		
12.49									
12.591	6^+								
12.683	5^-			12.6					
12.730	4^+								
12.83									
12.919									

[a] Because of low yield and high background, no angular distributions extracted, S_α only estimated from few angle cross sections.

[b] Value of S_α given under the assumption of $2N + L = 8$. Since these states are of core excited nature, $2N + L = 6$ and 4 must be included. Therefore the given values are the lower limits. Calculations with pure $2N + L = 6(4)$ would increase the S_α value by a factor of about 10(40), respectively.

[c] The 1^- states at 8.694 and 8.848 MeV are not resolved from each other and from the 6^+ state at 8.777 MeV. The S_α value for the sum of the 1^- states is estimated to be 0.09 (LOLA), 0.13 (DWUCK5); see text for discussion, and Fig. 5.

[d] State of core excited nature; see Ref. 35 and footnote b.

[e] State of core excited nature; see Ref. 34 and footnote b.

[f] Poor or bad fit of the DWBA calculation to the experimental data. Consequently, the S_α value is rather uncertain.

The extracted spectroscopic factors are given in Table I, where the present and previous experimental results as well as the results of the shell-model calculations are collected. The spectroscopic factors are normalized to the ground-state transition spectroscopic factor which itself is given relative to the ${}^{20}\text{Ne} \rightarrow {}^{16}\text{O}_{g.s.}$ transition spectroscopic factor.[44] As can be seen from the table, generally both of the computer codes (LOLA, DWUCK5) employed for analyzing the data, and used as described above, give essentially the same spectroscopic results.

For the members of the ground-state band (0^+, 2^+, 4^+, 6^+, and 8^+ at 0.0, 1.634, 4.248, 8.777, and 11.949 MeV, respectively) a rather satisfactory agreement between the present results and the shell-model calculations is observed. In general the experimental relative spectroscopic factors for the excited states are larger than the theoretical ones, but only by a factor of up to 2.

The 4^+ state of the second 0^+ band (0^+, 2^+, and 4^+ at 6.724, 7.421, and 9.99 MeV, respectively) is predicted[26] to have the strongest spectroscopic factor among the member's of this band. In fact, for the 0^+ and 2^+ states only upper limits could be estimated from counting rates observed in several spectra in the particular excitation energy range. The statistics were too small and the back-

ground was too high to extract reliable angular distributions for the 0^+ and 2^+ state of the 0_2^+ band. A peak was observed at 10 MeV excitation energy. The angular distribution is shown in the upper part of Fig. 7. A total angular momentum transfer of $L = 4$ (solid curve) seems quite reasonable when comparing these data to the data extracted for the excitation of the 4^+ member of the ground-state band (see Fig. 5). Again the experimental spectroscopic factor is larger than the predicted value,[26] as can be seen in Table I.

Figure 7 shows further the angular distributions for peaks observed at 7.2 and 7.8 MeV, which are fairly well fitted by an incoherent summation of $L = 0$ plus $L = 3$ and by pure $L = 2$ DWBA calculations, respectively. Probably, contributions resulting from members of the 0_3^+ core excited band are observed here. Since the various particle-hole configurations (mixture of contributions from 4p-0h, 6p-2h, and 8p-4h) are insensitive to the angular distribution shape but drastically sensitive to the cross section amplitude, the extraction of a spectroscopic factor remains inconclusive, as long as no good theoretical calculations or wave function descriptions for these states are available.

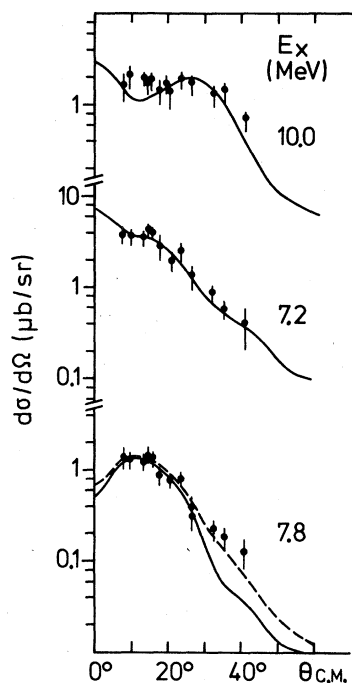Angular distributions resulting from peaks which are located in excitation energy ranges of expected

FIG. 7. Angular distributions of the $(d, {}^6\text{Li})$ reaction for final states in ${}^{20}\text{Ne}$. Solid lines: calculations done with the code LOLA, see text. Dashed lines: calculations done with the code DWUCK5, see text. Curves obtained assuming the observed peaks being due to final states with spin and parity as 10.0 MeV = 4^+, 7.2 MeV = 3^- plus 0^+, 7.8 MeV = 2^+; see Table I.

FIG. 8. Angular distributions of the $(d, {}^6\text{Li})$ reaction for final negative parity states in ${}^{20}\text{Ne}$; see Table I and text.

negative parity states are shown in Fig. 8. The 3^- state at 5.63 MeV excitation energy is by far the strongest. The observed angular distribution is not quite reproduced by a pure $L = 3$ transfer calculation (dotted line). The fit of the DWBA curve to the data improves when including some $L = 1$ contributions (solid line $L = 3$ plus $L = 1$), due to the known[40] 1^- state at 5.784 MeV excitation energy. The experimental angular distribution shape of the 5^- state at 8.4 MeV is not reproduced by the DWBA calculation. Experimentally observed yields resulting from the population of the unnatural parity states 2^- at 4.97 MeV, 4^- at 6.95 MeV, and 6^- at 10.6 MeV (the latter probably involves strengths from other nuclear states as well; see Table I) are not expected to be strongly excited in a one-step direct process. No attempts have been made to extract spectroscopic strengths for these states. Coupled channel calculations are in preparation and will be a topic of further investigations.

Angular distributions of peaks observed in the ${}^{24}\text{Mg}(d, {}^6\text{Li}){}^{20}\text{Ne}$ reaction which could not be associated uniquely to a single known spin and parity assignment are collected in Fig. 9. Part
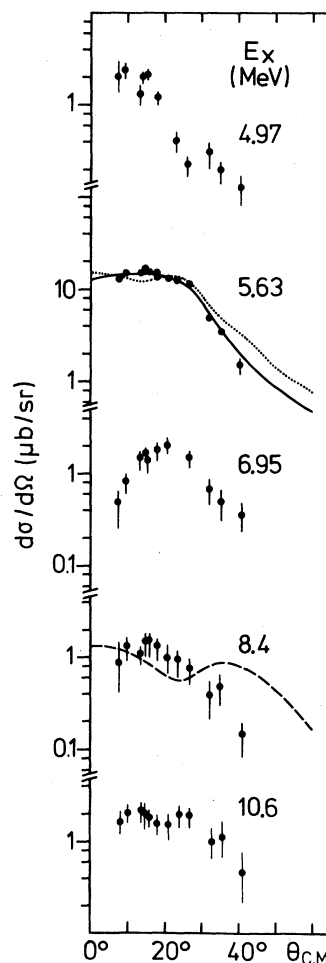
of the yield for the peak observed at 9.4 MeV excitation energy could be due to the excitation of a 2^+ final state; see Table I. However, the theoretical DWBA fit is not convincing. The yield of the peak observed at 10.3 MeV should be due to contributions of populating the 3^- and 5^- states at 10.403 and 10.261 MeV, respectively. Since the angular distribution shape is structureless the ratio of the strengths for these states cannot be well determined experimentally.

At the excitation energy range of 10.9 ± 0.2 MeV several levels are known[40] with spins ranging from 0 to 4. A superposition of yields for excitation of a 2^+ and 4^+ state seems to best reproduce the experimental data, as given in Fig. 9 and Table I; further contributions, however, as, e.g., an excitation of a 3^- state (see Ref. 35), cannot be excluded.
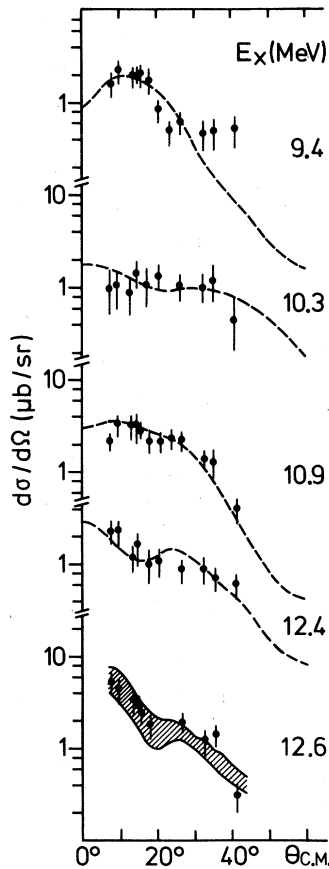
In Fig. 9 the angular distribution of the peak

FIG. 9. Angular distributions of the $(d, {}^{6}\text{Li})$ reaction for final states in ${}^{20}\text{Ne}$. See caption of Fig. 7. Here 9.4 MeV = 2^+, 10.3 MeV = 3^- plus 5^-, 10.9 MeV = 2^+ plus 4^+, 12.4 MeV = 3^-, 12.6 MeV; see text.

observed at 12.4 MeV is compared to a FR-DWBA calculation (DWUCK5)[46] assuming the excitation of a 3^- state. The fit is rather poor, but it is the best possible fit for a single final state. If this interpretation is correct, the tentative assignment for the 12.39 MeV 3^- state as a $T = 1$ state[40] seems questionable. The question arises, however, whether an experimental angular distribution shape is really typical for a unique spin and parity assignment. It will be shown in the case of the ${}^{26}\text{Mg}(d, {}^{6}\text{Li}){}^{22}\text{Ne}$ reaction that two different experimental angular distribution shapes are observed for the excitation of the first two 4^+ states. The envelope of the angular distribution shape for the excitation of the first 4^+ state at 3.36 MeV in ${}^{22}\text{Ne}$ (see Fig. 11) is superimposed on to the angular distribution for the excitation of the 12.6 MeV state observed in ${}^{20}\text{Ne}$ and shown in Fig. 9. This way it appears that, e.g., an empirical 4^+ assignment for the state at 12.6 MeV cannot be excluded, even though an appropriate DWBA curve would not fit the data.

B. The ${}^{26}\text{Mg}(d, {}^{6}\text{Li}){}^{22}\text{Ne}$ reaction

The natural, positive parity levels of ${}^{22}\text{Ne}$ (Refs. 41, 51) are displayed in Fig. 10. The open circles represent the experimentally known levels, the full circles the theoretically predicted ones.[26] Up to an excitation energy of about 7 MeV there seems to be a unique one to one correspondence between experimentally known and theoretically calculated levels. The members of the ground-state band are connected by straight lines. Further band structures, as they are known, e.g., in the case of the ${}^{20}\text{Ne}$ nucleus, are not established.[52]

The extracted angular distributions of the ${}^{26}\text{Mg}(d, {}^{6}\text{Li}){}^{22}\text{Ne}$ reaction are shown in Figs. 11 and 12. The DWBA and the experimental angular distribution shape for the ground-state transition (Fig. 11) are in good agreement. Two angular distributions are shown in Fig. 11 which are due to the excitation of known 2^+ states in the final nucleus ${}^{22}\text{Ne}$. However, the shape of the angular distribution for the excitation of the second 2^+ state at 4.46 MeV is well reproduced by the DWBA calculation, whereas the data for the first 2^+ state at 1.27 MeV show a relative enhancement of the cross sections for reaction angles larger than $30°$. The same tendency is observed in the case of the excitation of the first 2^+ state in the ${}^{24}\text{Mg}$ $(d, {}^{6}\text{Li}){}^{20}\text{Ne}$ reaction; see Fig. 5, the 1.63 MeV
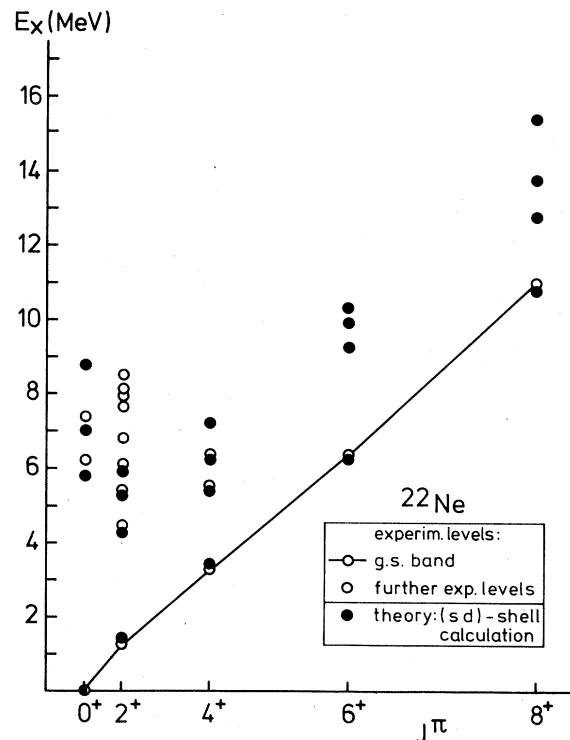

FIG. 10. Positive natural parity states in ${}^{22}\text{Ne}$; experimentally known levels and theoretically predicted ones.
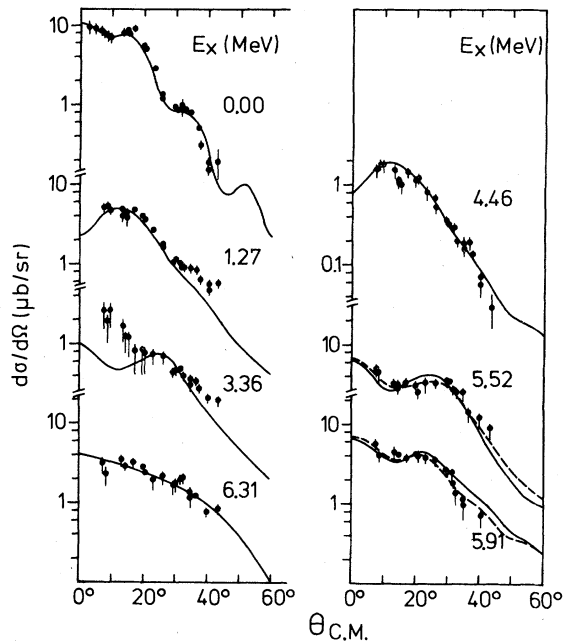
FIG. 11. Angular distributions of the $(d, {}^6\text{Li})$ reaction for final states in ${}^{22}\text{Ne}$. See text for discussion.

2^+ state.

As mentioned before, the angular distribution shape for the first 4^+ state in ${}^{22}\text{Ne}$ at 3.36 MeV excitation energy deviates significantly from the one-step DWBA calculation. Consequently, the extracted experimental spectroscopic factor, as given in Table II, is rather meaningless. It is interesting to note that the theoretical spectroscopic factor predicted[26] for the population of this 4^+ state from the ${}^{26}\text{Mg}$ ground state is very small.
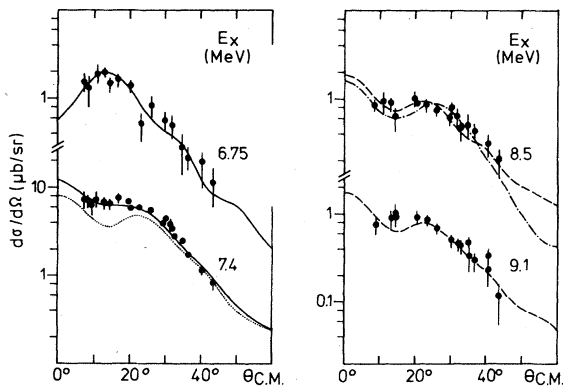

FIG. 12. Angular distributions of the $(d, {}^6\text{Li})$ reaction for final states in ${}^{22}\text{Ne}$. See caption of Fig. 7. The dotted line (7.4 MeV) is a DWBA calculation for a pure 3^- final state. The solid line includes contributions for a 0^+ final state; see Table II. Dashed and dashed-dotted lines (8.5 MeV) denote 3^- and 4^+ final state assumptions, respectively.

The angular distribution for the second 4^+ state in ${}^{22}\text{Ne}$ at 5.52 Mev excitation energy is rather well reproduced by the DWBA calculations, slightly favoring the DWUCK5[46] fit (dashed line) which was employed as described above.

The angular distribution extracted for the peak observed at 6.31 MeV excitation energy is shown in Fig. 11. This peak is not clearly resolved from nearby groups; see Fig. 2. In addition, four nuclear states (0^+, 2^+, 4^+, and 6^+) are known within the experimental width of the 300 keV FWHM energy resolution. The present result seems to indicate that the spectroscopic strength for the excitation of the 6^+ state at 6.311 MeV is underpredicted by the shell-model calculation,[26] whereas a good agreement is observed between the experimental and theoretical spectroscopic factors for the other states at around 6.31 MeV. The analysis is based on the assumption that the angular distributions of the individual experimental transitions are fitted by the appropriate DWBA calculations. In the case of the 5.91 MeV state the data agree rather well with the DWBA calculations for a 3^- final state.

Figure 12 presents the data at excitation energies between 6.7 and 9.1 MeV. In the case of the 6.75 and 9.1 MeV states the theoretical curves for final states with spin and parity of 1^- and 3^-, respectively, describe the data satisfactorily. The major part of the yield resulting from the excitation of the peak at 7.4 MeV seems to be due to a 3^- final state (dotted line); some incoherently added 0^+ contribution (solid line) improves the fit. Finally, in the case of the 8.5 MeV state no distinction between a 3^- (dashed DWBA curve) or a 4^+ (dashed-dotted DWBA curve) assignment can be made. The 5^- assignment of Ref. 35, however, does not agree with the present data.

DISCUSSION AND SUMMARY

The $(d, {}^6\text{Li})$ reaction at $E_d = 80$ MeV has been measured on the isotopes ${}^{24}\text{Mg}$ and ${}^{26}\text{Mg}$. The data were analyzed in the FR-DWBA formalism up to excitation energies of 12.6 and 9.1 MeV for the final nuclei ${}^{20}\text{Ne}$ and ${}^{22}\text{Ne}$, respectively. Further peaks are observed at higher excitation energies up to about 20 MeV (see Figs. 1 and 2), which might have their counterparts in the strong yield observed in (α, α') experiments on ${}^{20}\text{Ne}$ and ${}^{22}\text{Ne}$ between the low lying levels and the $E2$ giant quadrupole resonance.[53, 54] Further experimental investigations are necessary for confirmation.

In Tables I and II the present experimental spectroscopic results for the ${}^{24}\text{Mg}(d, {}^6\text{Li}){}^{20}\text{Ne}$ and ${}^{26}\text{Mg}(d, {}^6\text{Li}){}^{22}\text{Ne}$ reactions, respectively, are compared to shell-model calculations[26] and to

TABLE II. Alpha-spectroscopic factors S_α for final states in ^{22}Ne excited by the $(d, {}^{6}Li)$ reaction. Values are presented from (i) sd-shell model calculations, (ii) the present analysis, and (iii) previous results. The S_α value for the ground-state transition is given relative to the ^{20}Ne $\rightarrow {}^{16}$O ground-state transition S_α factor. The others are relative to the ^{26}Mg$(d, {}^{6}Li){}^{22}$Ne ground-state transition S_α factor.

| Theory | | Theory | | Present experiment | | | Previous experiments | |
E_x(MeV) Ref. 41	J^π	E_x(MeV) Ref. 26	S_α	E_x(MeV)	S_α LOLA	S_α DWUCK5	S_α Ref. 35	S_α Ref. 32
0.000	0⁺	0.00	0.43	0.00	0.37	0.46		
1.275	2⁺	1.39	0.15	1.27	0.65	0.66	0.80	1.80
3.357	4⁺	3.42	0.02	3.36	0.15 [f]	0.15 [f]	0.17	
4.457	2⁺	4.28	0.04	4.46	0.21	0.19	0.13	
5.148	2⁻							
5.336	1⁺							
5.365	2⁺	5.27	<0.01				0.19	
5.523	4⁺	5.40	0.69	5.52	0.89	0.75	0.98	
5.641	3⁺							
5.910	3⁻			5.91	2.44	2.93	1.38	
6.115	2⁺	5.91	0.10		0.07	0.08	0.09	
6.237	0⁺	5.77	0.08		0.07	0.08	0.10	
6.311	6⁺	6.26	0.03	6.31	0.45	0.24	0.8	
6.345	4⁺	6.23	0.18		0.20	0.24	0.3	
6.636	(2,3)⁺							
6.691	1⁻			6.75	0.50 [c]	0.82 [c]	0.24	
6.817	2⁺						0.11	
6.854	1⁺							
6.904	(0,1)⁺							
7.052	1⁻						0.06	
7.341	(3,4)⁺	7.21	0.03 [a]					
7.342	0⁺	6.99	0.03		<0.2 [d]			
7.406	(1,3)⁻			7.4	2.1	≤4.3 [e]	2.40 [b]	
7.423	(3,5)⁻							
(7.470)								
7.489	1⁻							
7.644	2⁺						0.12	
7.664	2⁻							
7.721	3⁻						0.06	
7.924	2⁺						0.07	
8.081	(2—4)⁺							
8.131	2⁺						0.12	
8.162	3							
8.382	(3⁻4⁺)					g, h		
8.452	5⁻					if <0.2		
8.491	2⁺			8.5				0.73
8.548	(0—4)⁺							
8.592								
8.737	3⁻							0.13
8.861	(0—4)⁺							
8.902	(0—3)⁻							
8.979								
9.040								
9.097	(1—3)⁻			9.1		0.45		
9.170								
9.223								
9.250								

[a]Theoretical S_α factor for 4⁺ final state at 7.21 MeV.

[b]Final state identified as 3⁻ state; see Ref. 35.

[c]Spectroscopic contributions from an excitation of a 2⁺ final state cannot be excluded.

[d]Maximum S_α factor for 0⁺ final-state assumption; however, 1⁻ contribution cannot be excluded; see Figs. 3 and 12.

[e]S_α factor for 7.4 MeV state being a pure 3⁻ state. The fit improves if 1⁻ components are included in the DWBA calculations and would lead to S_α (3⁻): 3.2 and S_α (1⁻): 1.1; see footnote d.

[f]Poor or bad fit of the DWBA calculation to the experimental data. Consequently, the S_α value is rather uncertain.

[g]S_α factor <0.2 if the 8.5 MeV peak is due to a 3⁻ final state; see Fig. 12.

[h]S_α factor <0.6 if the 8.5 MeV peak is due to a 4⁺ final state; see Fig. 12.

previous investigations.[32, 34, 35] Generally the
experimental results agree within fair limits
relative to each other. In some cases, however,
large deviations appear as, e.g., for the first
4^+ and 6^+ states in ^{20}Ne, where changes of the
experimental spectroscopic factor, by a factor
of 5 and more than 10 are observed. The reason
for such special cases might be that DWBA cal-
culations do not meet the actual reaction mecha-
nism process, e.g., as could be observed in the
case of the excitation of the first 4^+ state in ^{22}Ne.
On the other hand, it should be mentioned that in
some cases even the relative spectroscopic fac-
tors are sensitive to the parameters used in the
DWBA analysis, as can be seen, for example, for
the evaluation of the spectroscopic factor for the
1^- state in ^{22}Ne at 6.75 MeV extracted in the pre-
sent investigation (i) with the code LOLA[39] (ex-
ployed with no D-state contribution in the relative
α-$d \equiv {}^6$Li motion and with a constant ^{6}Li optical
potential), and (ii) with the code DWUCK5[46] (em-
ployed with D-state contributions in ^{6}Li and with
an energy dependence of the ^{6}Li optical potential).
A dependence of the absolute and relative spectro-
scopic factor on the bound-state radius parameter
has been pointed out earlier.[55] A possible flexi-
bility of the bound-state radius is discussed in the
present contribution.

The distribution of the experimental relative
spectroscopic strength for 3^- states in ^{20}Ne and
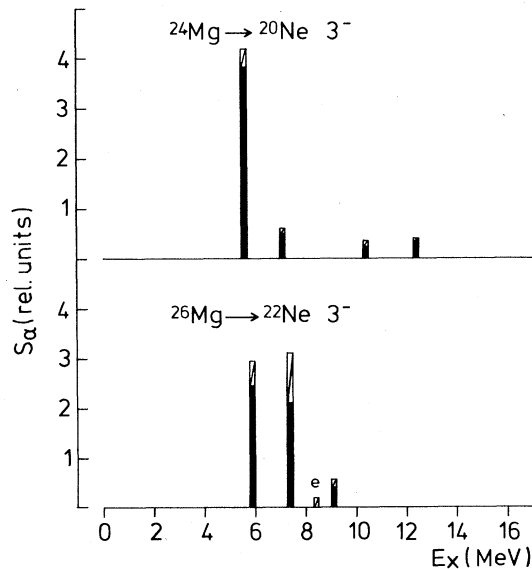^{22}Ne is shown in Fig. 13. About the same relative
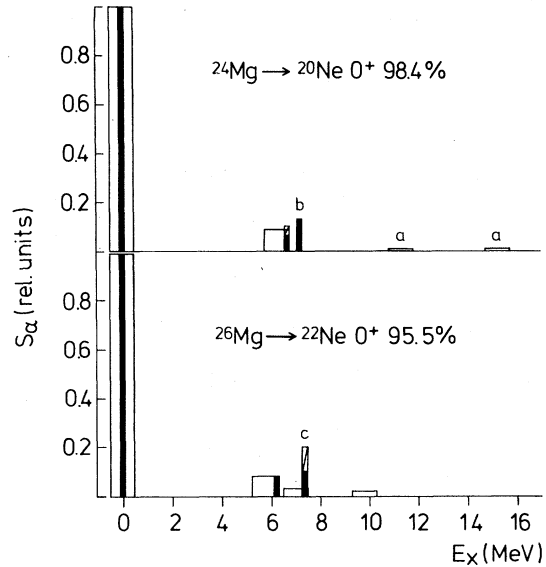

FIG. 14. Distribution of relative alpha transfer spec-
troscopic strength in ^{20}Ne and ^{22}Ne for 0^+ final states.
Legend: see Fig. 18. a: Theoretical spectroscopic
factor <1% of S_α for ground-state transition. b: Core
excited state. c: Spectroscopic factor is probably smal-
ler, see text.

FIG. 13. Disbribution of relative alpha transfer spec-
troscopic strength in ^{20}Ne and ^{22}Ne for 3^- final states.
Legend: see Fig. 18. e: $J^\pi = 3^-$ not clear; see text and
Fig. 16.

strength is found in both of the final nuclei, in
^{20}Ne concentrated rather strongly at 5.63 MeV, in
^{22}Ne distributed mainly on two states at 5.91 and
7.4 MeV excitation energy.

As can be seen from Tables I and II, the rela-
tive ground-state transition spectroscopic factors
agree well with the theoretical predictions, rela-
tive to the ^{20}Ne$\rightarrow$^{16}O$_{g.s.}$ transition strength.

In Figs. 14–18 the experimental spectroscopic
factors for positive natural parity states in the
final nuclei ^{20}Ne (upper part) and ^{22}Ne (lower part)
are compared to the results of shell-model cal-
culations,[26] normalized to unity for the ground-
state transitions. For the final nucleus ^{20}Ne 98.4%
of the expected theoretical 0^+ strength[26] (within
the limits of the full sd shell) is predicted at
excitation energies less than 16 MeV. Most of the
strength is concentrated in the ground-state trans-
ition, as in the case of the ^{26}Mg(d,^{6}Li)^{22}Ne reac-
tion, where 95.5% of the 0^+ strength lies at ex-
citation energies of less than 10 MeV. The agree-
ment between experimental and theoretical relative
spectroscopic factors for the 0^+ states is docu-
mented in Fig. 14, noting that the experimental
spectroscopic factor for the state at 7.2 MeV (b)
in ^{20}Ne contains p-shell contributions and con-
sequently is not predicted by the sd-shell model
calculations, and noting that the value of the ex-
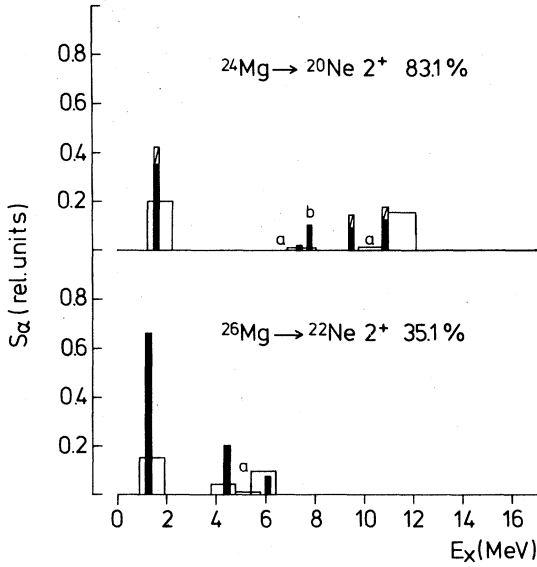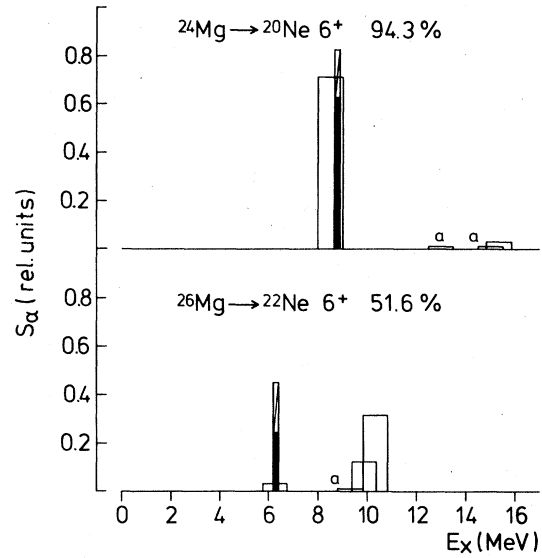perimental spectroscopic factor for the state at

FIG. 15: Distribution of relative alpha transfer spectroscopic strength in ^{20}Ne and ^{22}Ne for 2^+ final states. Legend: see Fig. 18. a: Theoretical spectroscopic factor <1% of S_α for ground-state transition. b: Core excited state.

FIG. 17. Distribution of relative alpha transfer spectroscopic strength in ^{20}Ne and ^{22}Ne for 6^+ final states. Legend: see Fig. 18. a: Theoretical spectroscopic factor <1% of S_α for ground-state transition.

7.4 MeV (c) in ^{22}Ne is rather unreliable because of the unresolved 3^- and especially 1^- states; see Table II.

The experimental and theoretical spectroscopic factors for 2^+ final states are shown in Fig. 15. Generally the experimental values are larger than

the theoretical ones. Especially for the transition to the first and second 2^+ states in ^{22}Ne, it seems that more than the predicted[26] 35.1% of the 2^+ strength is concentrated at low excitation energies.

Except for the first 4^+ state at 3.36 MeV in ^{22}Ne, the relative experimental spectroscopic strength

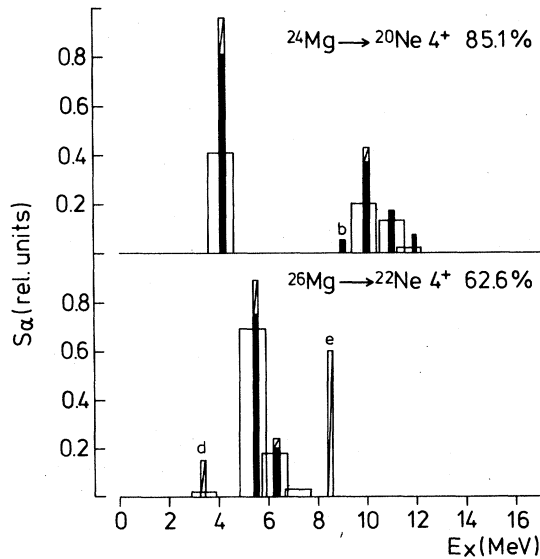FIG. 16: Distribution of relative alpha transfer spectroscopic strength in ^{20}Ne and ^{22}Ne for 4^+ final states. Legend: see Fig. 18. b: Core excited state. d: Bad DWBA fit to data, see text. e: $J^\pi = 4^+$ not clear, see text.
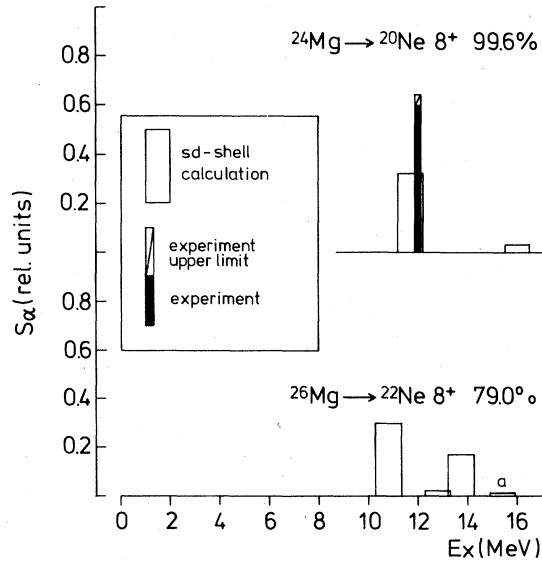

FIG. 18. Distribution of relative alpha transfer spectroscopic strength in ^{20}Ne and ^{22}Ne for 8^+ final states. a: Theoretical spectroscopic factor <1% of S_α for ground-state transition.

distribution for 4⁺ final states, as shown in Fig. 16, agrees rather well to the predicted values, again the experimental factors being somewhat larger than the theoretical ones. The direct one-step contribution for the excitation of the first 4⁺ state in ^{22}Ne seems to be very small, as discussed above; see Fig. 11. The peak observed at 8.5 MeV excitation energy in ^{22}Ne could not be uniquely identified as being due to a 4⁺ state; consequently, the experimental spectroscopic factor (e) serves only as a possible upper limit.

Experimental and theoretical results agree that nearly all spectroscopic strength for 6⁺ final states in ^{20}Ne is concentrated in the 6⁺ member of the ground-state band, as shown in Fig. 17. As in the case of 4⁺ final states in ^{22}Ne, the first 6⁺ state in ^{22}Ne is predicted[20] to be rather weakly excited. Since the experimental spectroscopic factor for the 6⁺ state was extracted by a best fit procedure superposing four DWBA curves, its value is rather uncertain, especially since it is not known whether the individual experimental angular distribution shape would agree with a 6⁺ final-state one step DWBA calculation. In the present experiment, 6⁺ strength could not be identified at higher excitation energies. A better energy resolution would be necessary to study the high level density region.

In ^{22}Ne no 8⁺ state could be identified experimentally. The experimental spectroscopic factor for the 8⁺ state in ^{20}Ne at 11.9 MeV again is larger than the predicted one, but only by a factor of 2; see Fig. 18 and Table I.

In summary, rather good agreement is observed between sd-shell model predictions[26] and present experimental values of relative spectroscopic factors. The average experimental values

for excited states are somewhat larger than the theoretical ones, relative to the ground-state transition. This result might be due to a physically larger reduced matrix element of the individual four-nucleon creation operator leading from nucleus A to excited states of nucleus A-4, than predicted by the shell-model calculations.[26]

It should be mentioned, however, that the assumed direct one-step reaction process might not meet the actual physical conditions. This hypothesis is supported by the experimental results for the low lying 4⁺ states. In ^{22}Ne the experimental angular distribution of the first 4⁺ state cannot be fitted by DWBA calculations; the extracted "spectroscopic factor" is a factor of 10 larger than the predicted one. In ^{20}Ne the experimental angular distribution of the first 4⁺ state is poorly fitted by DWBA calculations; the extracted spectroscopic factor is about a factor of 2 larger than the predicted one. Finally, the experimental angular distribution of the second 4⁺ state in ^{22}Ne is well fitted by DWBA calculations—the extracted spectroscopic factor is only 10–30% larger than the predicted relative value.

Further investigations of the reaction mechanism process seem to be necessary for answering the question whether the rather small deviations between experimental and theoretical spectroscopic factors for excited states are significant in the ^{24}Mg($d,^6$Li)^{20}Ne and ^{26}Mg($d,^6$Li)^{22}Ne reactions.

ACKNOWLEDGMENTS

[1]K. Bethge, Annu. Rev. Nucl. Sci. 20, 255 (1970).

[2]W. v. Oertzen, *Clustering Phenomena in Nuclei*, College Park, Maryland, 1975, edited by D. A. Goldberg, J. B. Marion, and S. J. Wallace (National Technical Information Service, U. S. Dept. of Commerce, Springfield, Va., 1975), Vol. II, p. 367.

[3]V. Gillet, see Ref. 2, p. 23.

[4]F. D. Becchetti, *Clustering Aspects of Nuclear Structure and Nuclear Reactions, Winnipeg, 1978*, Proceedings of the Third International Conference on Clustering Aspects of Nuclear Structure and Nuclear Reactions, edited by W. T. H. van Oers, J. P. Svenne, J. S. C. McKee, and W. R. Falk (AIP, New York, 1978), p. 308.

[5]H. W. Fulbright, Nukleonika 22, 235 (1977).

[6]A. Arima, see Ref. 4, p. 1.

[7]R. Y. Cusson, J. Gomez del Campo, and H. W. Melder, see Ref. 4, p. 35.

[8]P. E. Hodgson, *Nuclear Heavy-Ion Reactions* (Clarendon, Oxford, 1978).

[9]M. Harvey, *Advances in Nuclear Physics*, edited by M. Baranger and E. Vogt (Plenum, New York, 1968), Vol. I.

[10]J. P. Draayer, Nucl. Phys. A237, 157 (1975); M. Conze, Ph.D. thesis, Technische Hochschule Darmstadt, 1976 (unpublished).

[11]M. Ichimura, A. Arima, E. C. Halbert, and T. Terasawa, Nucl. Phys. A204, 225 (1973).

[12]K. T. Hecht and D. Braunschweig, Nucl. Phys. A244, 365 (1975).

[13]A. Bohr, in *Proceedings of the International Symposium on Nuclear Structure, Dubna, 1968* (IAEA, Vienna, 1968), p. 179 and O. Nathan, p. 191.

[14]D. R. Bes and R. A. Broglia, Nucl. Phys. A80, 289 (1966); A. Bohr and B. R. Mottelson, *Nuclear Structure* (Benjamin, New York, 1975), Vol. II.

[15]R. A. Broglia, L. Ferreira, P. D. Kunz, H. Sofia, and A. Vitturi, Phys. Lett. 79B, 351 (1978).

[16]A. Arima and F. Iachello, Ann. Phys. (N.Y.) 99, 253 (1976); Phys. Rev. C 16, 2085 (1977).

[17]C. L. Bennett and H. W. Fulbright, Phys. Rev. C 17, 2225 (1978).

[18]K. Wildermuth and Th. Kanellopoulos, Nucl. Phys. 7, 150 (1958).

[19]B. Buck, C. B. Dover, and J. P. Vary, Phys. Rev. C 11, 1803 (1975).

[20]T. Matsuse and M. Kamimura, Prog. Theor. Phys. 49, 1765 (1973).

[21]P. Kramer, see Ref. 2, p. 56.

[22]M. Kamimura, T. Matsuse, and K. Takada, Prog. Theor. Phys. 47, 1537 (1972).

[23]K. T. Hecht, Phys. Rev. C 16, 2401 (1977).

[24]T. Fliessbach and P. Manakos, J. Phys. G 3, 643 (1977).

[25]W. Chung, J. van Hienen, B. H. Wildenthal, and C. L. Bennett, Phys. Lett. 79B, 381 (1978).

[26]W. Chung and B. H. Wildenthal (unpublished); W. Chung, Ph.D. thesis, Michigan State University, 1976 (unpublished).

[27]F. W. Slee, Ph.D. thesis, University of Washington, 1966 (unpublished).

[28]J. B. Gerhart, P. F. Mizera, and F. W. Slee, Ann. Rep. University Washington, 1966 (unpublished), p. 36.

[29]R. L. McGrath, J. Cerny, B. G. Harvey, and D. L. Hendric, Bull. Am. Phys. Soc. 15, 629 (1970); R. L. McGrath, D. L. Hendric, E. A. McClatchie, B. G. Harvey, and J. Cerny, Phys. Lett. 34B, 289 (1971).

[30]J. Reder, Diplomarbeit, thesis, Max-Planck-Institut für Kernphysik, Heidelberg, 1974 (unpublished).

[31]A. Djaloeis, D. Ingham, H. Kelleter, O. Aspelund, and C. Mayer-Böricke, Z. Phys. 260, 133 (1974).

[32]J. D. Cossairt, R. D. Bent, A. S. Broad, F. D. Becchetti, and J. Jänecke, Nucl. Phys. A261, 373 (1976).

[33]J. R. Comfort, W. J. Braithwaite, J. R. Duray, H. T. Fortune, W. J. Courtney, and H. G. Bingham, Phys. Lett. 40B, 456 (1978).

[34]H. T. Fortune, W. J. Courtney, J. R. Comfort, W. J. Braithwaite, J. R. Duray, and A. A. Pilt, Phys. Rev. C 17, 1955 (1978).

[35]J. C. Vermeulen, A. G. Drentje, H. T. Fortune, J. F. A. van Hienen, L. W. Put, R. R. de Ruyter van Steveninck, R. H. Siemssen, and A. v. d. Woude, KVI annual report, University Groningen, 1978, p. 19; J. C. Vermeulen, Ph.D. thesis, University Groningen, 1979 (unpublished).

[36]R. G. H. Robertson, S. Martin, W. R. Falk, D. Ingham, and A. Djaloeis, Phys. Rev. Lett. 32, 1207 (1974).

[37]W. Oelert, A. Djaloeis, C. Mayer-Böricke, P. Turek, and S. Wiktor, Nucl. Phys. A306, 1 (1978).

[38]J. R. Comfort, ANL Physics Division Informal Report No. PHY-1970 B, 1970 (unpublished); P. Sprink and J. R. Erskine, ANL Physics Division Informal Report No. PHY-1965 B, 1965 (unpublished).

[39]R. M. De Vries, Finite-Range DWBA code LOLA; Phys. Rev. C 8, 951 (1973).

[40]F. Ajzenberg-Selove, Nucl. Phys. A300, 148 (1978); D. A. Bromley, Nucl. Instrum. Methods 146, 1 (1977).

[41]F. Ajzenberg-Selove, Nucl. Phys. A310, 46 (1978).

[42]J. D. Childs, W. W. Daehnick, and M. J. Spisak, Phys. Rev. C 10, 217 (1974) and University of Pittsburgh, report of current research, 1976–1977 (unpublished), p. 50.

[43]L. T. Chua, F. D. Becchetti, J. Jänecke, and F. L. Milder, Nucl. Phys. A273, 243 (1976).

[44]W. Oelert, W. Chung, M. Betigeri, A. Djaloeis, C. Mayer-Böricke, and P. Turek, Phys. Rev. C 20, 459 (1979).

[45]W. Oelert, M. Betigeri, W. Chung, A. Djaloeis, C. Mayer-Böricke, and P. Turek, Nucl. Phys. A329, 192 (1979).

[46]P. D. Kunz, Finite-Range DWBA code DWUCK5, University of Colorado, Boulder (unpublished).

[47]M. F. Werby, M. B. Greenfield, K. W. Kemper, D. L. McShan, and S. Edwards, Phys. Rev. C 8, 106 (1973).

[48]C. L. Bennett, Nucl. Phys. A284, 301 (1977).

[49]A. Arima and S. Yoshida, Phys. Lett. 40B, 15 (1972).

[50]M. C. Lee and R. Y. Cusson, Phys. Rev. Lett. 29, 1525 (1972).

[51]C. Broude, W. G. Davies, J. S. Forster, and G. C. Ball, Phys. Rev. C 13, 953 (1976).

[52]E. M. Szanto, A. Szanto de Toledo, H. V. Klapdor, M. Diebel, J. Fleckner, and U. Mosel, Phys. Rev. Lett. 42, 622 (1979).

[53]K. T. Knöpfle, G. J. Wagner, A. Kiss, M. Rogge, C. Mayer-Böricke, and Th. Bauer, Phys. Lett. 64B, 263 (1976).

[54]C. Sükösd, private communication.

[55]W. Oelert, M. Betigeri, W. Chung, A. Djaloeis, C. Mayer-Böricke, and P. Turek, Verh. Dtsch. Phys. Ges. 14, 849 (1979).